Numer. Math. (2008) 111:81–108
DOI 10.1007/s00211-008-0174-6

Numerische Mathematik

Convergence analysis of sectional methods for solving breakage population balance equations-I: the fixed pivot technique

Jitendra Kumar · Gerald Warnecke

Received: 6 November 2007 / Revised: 8 July 2008 / Published online: 19 August 2008

Abstract In this work we study the convergence of the fixed pivot techniques (Kumar and Ramkrishna Chem. Eng. Sci. **51**, 1311–1332, 1996) for breakage problems. In particular, the convergence is investigated on four different types of uniform and non-uniform meshes. It is shown that the fixed pivot technique is second order convergent on a uniform and non-uniform smooth meshes. Furthermore, it gives first order convergence on a locally uniform mesh. Finally the analysis shows that the method does not converge on a non-uniform random mesh. The mathematical results of convergence analysis are also validated numerically.

Mathematics Subject Classification (2000) 65R20

1 Introduction

Population balances for breakage are widely known in high shear granulation, crystallization, atmospheric science and many other particle related engineering problems. The temporal change of particle number density, $f(t,x) \geq 0$, of particles of volume $x \in \mathbb{R}_{>0}$ at time $t \in \mathbb{R}_{\geq 0}$ in a spatially homogeneous physical system undergoing breakage and aggregation processes is described by the following well known population balance equation, see e.g. [27]

$$\frac{\partial f(t,x)}{\partial t} = \int_x^\infty b(x,\epsilon) S(\epsilon) f(t,\epsilon)\, d\epsilon - S(x) f(t,x), \tag{1}$$

J. Kumar (✉) · G. Warnecke
Institute for Analysis and Numerics, Otto-von-Guericke University Magdeburg,
Universitätsplatz 2, 39106 Magdeburg, Germany
e-mail: jitendra.kumar@mathematik.uni-magdeburg.de

with

$$f(0,x) = f^{\text{in}}(x), \quad x \in]0,\infty[.$$

The first and second terms on the right hand side of the Eq. (4) are called the birth and death terms respectively. The breakage function $b(x,\epsilon)$ is the probability density function for the formation of particles of size x from particles of size ϵ. The selection function S describes the rate at which particles are selected to break. The breakage function has the following properties

$$\int_0^x b(\epsilon,x)\,d\epsilon = \nu(x), \quad b(\epsilon,x) = 0, \quad \text{for } \epsilon > x, \tag{2}$$

and

$$\int_0^x \epsilon b(\epsilon,x)\,d\epsilon = x. \tag{3}$$

The function $\nu(x)$ represents the number of fragments obtained from the breakage of particle of size x. For the total mass in the system to remain conserved during fragmentation events, b must satisfy the Eq. (3). It states that the total mass of the fragments equals the original mass when a particle of mass x breaks.

The mathematical results on existence and uniqueness of solutions of Eq. (1) can be found in [4,18,19,21,22] for rather general breakage and selection functions. However, for the sake of simplicity in our analysis we consider them to be twice continuously differentiable functions. The above PBE (1) can only be solved analytically for very simple forms of the breakage and selection functions, see [3,27,28]. This certainly leads to a discussion of numerical methods for solving PBE. Numerical methods fall into several categories: stochastic methods, [20,23], finite element methods, [5], moment methods [9,10], asymptotic solution techniques [11], and sectional methods, [12,13,16,17].

In the population balance equation (1) the volume variable x ranges from 0 to ∞. In order to apply a numerical scheme for the solution of the equation a first step is to fix a finite computational domain. In this work we consider the following truncated equation

$$\frac{\partial n(t,x)}{\partial t} = \int_x^{x_{\max}} b(x,\epsilon)S(\epsilon)n(t,\epsilon)\,d\epsilon - S(x)n(t,x), \tag{4}$$

with

$$n(0,x) = n^{\text{in}}(x), \quad x \in \Omega :=]0, x_{\max}[.$$

Here the variable $n(t, x)$ denotes the solution to the preceding truncated equation. The truncated equation has been discussed in the literature by various authors. For a detailed discussion on it readers are referred to [1,2,4,6].

The stochastic methods (Monte-Carlo) are very efficient for solving multi-dimensional population balance equations, since other numerical techniques become computationally very expensive in such cases. A wide variety of finite element methods, finite volume methods, weighted residuals, the method of orthogonal collocation and Galerkin's method are also used for solving breakage population balance equations. These methods may give very good prediction of number density but poor prediction of moments, see Kumar et al. [15]. Other disadvantages of using higher order methods include stability problems and higher computational cost. In the moment method, the population balance equation is transformed into a system of ODEs describing the evolution of the moments of the particle size distribution. The moment methods indeed predict very accurate the moments of the distribution but are unable to give precise information about the density distribution. In recent times, the sectional methods have become computationally very attractive because they do not only predict some selected moments of the distribution very accurately but also give satisfactory results for the complete density distribution.

Several sectional methods for breakage PBE have been proposed by Hill and Ng [7], Kumar and Ramkrishna [16,17], Kumar et al. [12,13] as well as Vanni [25]. A detailed review of sectional methods has been given by Vanni [26]. Among all sectional methods, the fixed pivot technique is the most widely used method these days due to its generality and robustness. The technique predicts the first two moments of the distribution very accurately. Despite the fact that the numerically calculated first two moments are fairly accurate, the fixed pivot technique consistently over-predicts the results of number density as well as its higher moments. A step to improve the fixed pivot technique by preserving all advantages of the existing sectional methods has been recently made by the authors in the cell average technique [12,13].

In the literature, the numerical analysis of sectional methods is missing and therefore the objective of this work is to perform some numerical analysis of sectional methods. In this work we mainly concentrate on the work of Kumar and Ramkrishna [16] as a first step. In the next article of this series we will give the numerical analysis of the cell average technique. The outline of this paper is as follows. Next section briefly presents a general idea of sectional methods as well as some useful definitions and theorems used in further analysis of these methods. The Sect. 3 presents the mathematical formulation of the fixed technique followed by the consistency, stability and convergence analysis. Numerical experiments are carried out in Sect. 4. Finally, some conclusions are made in the last section.

2 The sectional methods

The sectional methods can be described by the following general mathematical derivation. The sectional methods approximate the total number of particles in finite number of cells. As a first step, the continuous interval $\Omega :=]0, x_{\max}[$ is divided into small

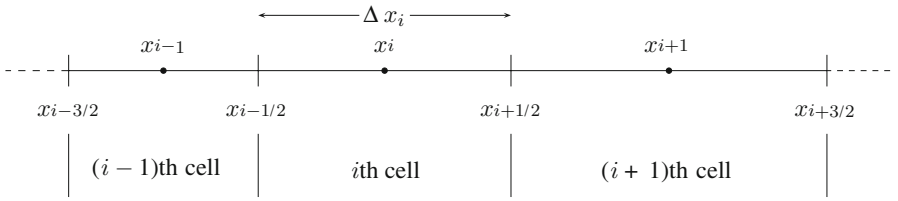

Fig. 1 A discretized size domain

number of cells

$$\Lambda_i :=]x_{i-1/2}, x_{i+1/2}], \quad i = 1, \ldots, I,$$

with

$$x_{1/2} = 0, \quad x_{I+1/2} = x_{\max}, \quad \Delta x_i = x_{i+1/2} - x_{i-1/2} \leq \Delta x.$$

The representative of each size, usually the center of each cell $x_i = (x_{i-1/2} + x_{i+1/2})/2$, is called pivot or grid point. Such type of partitioning of the spatial domain is known as *cell centered* representation of the mesh. A typical cell centered partitioning of the domain is shown in Fig. 1. The integration of the Eq. (4) over each cell yields a *semi-discrete* system in $\mathbb{R}^I$

$$\begin{aligned} \frac{d\mathbf{N}}{dt} &= \mathbf{B} - \mathbf{D}, \\ \mathbf{N}(0) &= \mathbf{N}^{\text{in}}. \end{aligned} \tag{5}$$

Here we consider $\mathbf{N}^{\text{in}}, \mathbf{N}, \mathbf{B}, \mathbf{D} \in \mathbb{R}^I$ whose semi-discrete ith components are defined as

$$N_i(t) = \int_{x_{i-1/2}}^{x_{i+1/2}} n(t, x)dx, \tag{6}$$

$$N_i^{\text{in}} = \int_{x_{i-1/2}}^{x_{i+1/2}} n^{\text{in}}(x)dx,$$

$$B_i = \int_{x_{i-1/2}}^{x_{i+1/2}} \int_{x}^{x_{I+1/2}} b(x, \epsilon)S(\epsilon)n(t, \epsilon)\, d\epsilon dx, \tag{7}$$

and

$$D_i = \int_{x_{i-1/2}}^{x_{i+1/2}} S(x)n(t, x)dx. \tag{8}$$

Various sectional methods for the numerical solutions of the Eq. (4) can be obtained from different choices of numerical approximations of B_i and D_i in terms of $N_i(t)$. Finally the sectional methods take the following spatially discretized form

$$\frac{d\hat{\mathbf{N}}}{dt} = \hat{\mathbf{B}}(\hat{\mathbf{N}}) - \hat{\mathbf{D}}(\hat{\mathbf{N}}), \tag{9}$$

$$\hat{\mathbf{N}}(0) = \mathbf{N}^{\text{in}}, \tag{10}$$

where $\hat{\mathbf{B}}, \hat{\mathbf{D}} \in \mathbb{R}^I$ are some functions of $\hat{\mathbf{N}}$. The ith component, $\hat{N}_i(t)$ of the vector $\hat{\mathbf{N}}$ is the numerical approximation of the total number in ith cell $N_i(t)$.

Before we proceed to next section to discuss the fixed pivot technique in details, it is convenient to review some useful theorems and definitions at this point, see Hundsdorfer and Verwer [8].

Definition 2.1 The *spatial truncation error* is defined by the residual left by substituting the exact solution $\mathbf{N}(t)$ into Eq. (9) as

$$\sigma(t) = \frac{d\mathbf{N}(t)}{dt} - \left(\hat{\mathbf{B}}(\mathbf{N}(t)) - \hat{\mathbf{D}}(\mathbf{N}(t))\right). \tag{11}$$

The scheme (9) is called consistent of order p if, for $\Delta x \to 0$,

$$\|\sigma(t)\| = \mathcal{O}(\Delta x^p), \quad \text{uniformly for all } t, \quad 0 \le t \le T.$$

Definition 2.2 The *global discretization error* is defined by $\epsilon(t) = \mathbf{N}(t) - \hat{\mathbf{N}}(t)$. The scheme (9) is called convergent of order p if, for $\Delta x \to 0$,

$$\|\epsilon(t)\| = \mathcal{O}(\Delta x^p), \quad \text{uniformly for all } t, \quad 0 \le t \le T.$$

Definition 2.3 The *logarithmic norm* of a matrix $\mathbf{A}$ in $\mathbb{C}^{m\times m}$ is defined as, see Hundsdorfer and Verwer [8],

$$\tilde{\mu}(\mathbf{A}) = \lim_{\tau\to 0} \frac{\|I + \tau\mathbf{A}\| - 1}{\tau}.$$

The logarithmic norm of a matrix $\mathbf{A}$ corresponding to certain $1-$norms on $\mathbb{R}^m$ is given by

$$\tilde{\mu}_1(\mathbf{A}) = \max_j \left(Re(a_{jj}) + \sum_{i\neq j} |a_{ij}| \right). \tag{12}$$

We denote the real part of a complex number z by $Re(z)$

The following theorem is useful for estimating the norm of the exponential of a matrix.

Theorem 2.4 *If* $\mathbf{A} \in \mathbb{C}^{m\times m}$ *and* $\omega \in \mathbb{R}$ *then we have*

$$\tilde{\mu}(\mathbf{A}) \leq \omega \iff \|e^{t\mathbf{A}}\| \leq e^{t\omega}, \quad \text{for all} \quad t \geq 0.$$

Proof See Hundsdorfer and Verwer [8], Chap. 1, Theorem 2.4. □

Now we include a useful definition and theorem for stability and convergence from Hundsdorfer and Verwer [8]. In case of pure breakage (linear) problem the Eq. (9) takes the following linear semi-discrete form

$$\frac{d\hat{\mathbf{N}}}{dt} = \mathbf{A}\hat{\mathbf{N}}(t). \tag{13}$$

The matrix $\mathbf{A}$ will be defined later.

Definition 2.5 The semi-discrete system (13) is called stable if we have on all grids

$$\|e^{t\mathbf{A}}\| \leq Ke^{\omega t} \quad \text{for} \quad 0 \leq t \leq T, \tag{14}$$

with constant $K \geq 1$ and $\omega \in \mathbb{R}$ both independent of Δx.

Theorem 2.6 (Hundsdorfer and Verwer [8]). *Consider the linear semi-discrete system* (13) *and assume the stability condition* (14) *is valid. Suppose further that* $\|\sigma(t)\| \leq C\Delta x^q$ *for* $0 \leq t \leq T$ *(consistency of order* q*) and* $\|\epsilon(0)\| \leq C_0\Delta x^q$ *with constant* C, $C_0 > 0$. *Then we have convergence of order* $p = q$ *with the error bounds*

$$\|\epsilon(t)\| \leq KC_0e^{\omega t}\Delta x^q + \frac{KC}{\omega}\left(e^{\omega t} - 1\right)\Delta x^q \quad \text{if } \omega \neq 0, \quad 0 \leq t \leq T,$$

and

$$\|\epsilon(t)\| \leq KC_0\Delta x^q + KCt\Delta x^q \quad \text{if } \omega = 0, \quad 0 \leq t \leq T.$$

Proof See Hundsdorfer and Verwer [8], Chap. 1, Theorem 4.1. □

Theorem 2.7 (Hundsdorfer and Verwer [8]). *The solution of the linear semi-discrete system* (13) *is non-negative iff*

$$a_{ij} \geq 0, \quad \text{for all,} \quad j \neq i.$$

Proof See Hundsdorfer and Verwer [8], Chap. 1, Theorem 7.2. □

Before proceeding to the next section it should be mentioned here that in this work we consider the following L_1 error norm

$$\|\mathbf{N}\| = \sum_{i=1}^{I} |N_i|.$$

3 The fixed pivot technique

The fixed pivot technique is also based on the idea of birth modification. According to Kumar and Ramkrishna [16], the Eq. (4) is modified to

$$\frac{d}{dt}\int_{x_{i-1/2}}^{x_{i+1/2}} n(t,x)dx \approx \int_{x_i}^{x_{i+1}} \lambda_i^+(x) \int_x^{x_{\max}} b(x,\epsilon)S(\epsilon)n(t,\epsilon)\,d\epsilon dx + \int_{x_{i-1}}^{x_i} \lambda_i^-(x) \int_x^{x_{\max}} b(x,\epsilon)S(\epsilon)n(t,\epsilon)\,d\epsilon dx - \int_{x_{i-1/2}}^{x_{i+1/2}} S(x)n(t,x)dx,$$

where

$$\lambda_i^{\pm}(x) = \frac{x - x_{i\pm1}}{x_i - x_{i\pm1}}. \tag{15}$$

Now substituting the number density approximation

$$n(t,x) \approx \sum_{i=1}^{I} N_i(t)\delta(x - x_i),$$

into the preceding equation, we obtain the following discretized equation

$$\frac{dN_i(t)}{dt} = \sum_{k=i}^{I} \eta_{ik}S(x_k)N_k(t) - S(x_i)N_i(t), \quad i = 1,\ldots,I. \tag{16}$$

Here the function η is described by

$$\eta_{ik} = \int_{x_i}^{x_{i+1}} \lambda_i^+(x)b(x,x_k)\,dx + \int_{x_{i-1}}^{x_i} \lambda_i^-(x)b(x,x_k)\,dx, \quad i,k = 1,\ldots,I,\ k \geq i.$$

The first and second integral terms reduce to zero for $i = k$ and $i = 1$, respectively. Note that the first term is zero for $i = k$ due the the property (2). In the rest of the paper we set $S_i = S(x_i)$. The above system of ordinary Eq. (16) can be written in the matrix form (13) with

$$\mathbf{A} = \begin{bmatrix} \eta_{11}S_1 - S_1 & \eta_{12}S_2 & \ldots & \eta_{1I}S_I \\ 0 & \eta_{22}S_2 - S_2 & \ldots & \eta_{2I}S_I \\ . & & & . \\ . & & & . \\ 0 & 0 & \ldots & \eta_{II}S_I - S_I \end{bmatrix}. \tag{17}$$

The fundamental concept behind the fixed pivot technique can be summarized as follows. Suppose a new particle of a size which is not a representative of any cell appears due to breakage of larger particles. The particle has to be divided to neighboring representatives in such a way that number and mass are conserved. In this process numerical diffusion is of course possible due to the assignment of particles to the representatives to whom they do not really belong. Nevertheless, quite satisfactory results can be obtained by this technique. Moreover, we will see later that the fixed pivot technique is a zero order method on non-uniform random mesh for breakage problems. Let us first check the positivity of the solution by the fixed pivot technique.

Proposition 3.1 *The numerical solution by the fixed pivot technique is non-negative.*

Proof Theorem 2.7 directly implies non-negativity of the solution since $a_{ij} \geq 0$ for all $j \neq i$ in the matrix (17). □

3.1 Consistency

We now consider a fundamental lemma useful for investigating the consistency of the fixed pivot technique. We take $\mathcal{C}^2([a, b])$ to be the two times continuously differentiable functions on $]a, b[$ with finite limits of the functions and their first as well as second derivatives at a and b.

Lemma 3.2 *Consider a function $f(x) \in \mathcal{C}^2([0, x_{max}])$ and a cell centered partitioning of the continuous domain $0 = x_{1-1/2} < \cdots < x_{i-1/2} < x_{i+1/2} < \cdots < x_{I+1/2} = x_{max}$ with $x_i = (x_{i-1/2} + x_{i+1/2})/2$ and $\Delta x \geq \Delta x_i = (x_{i+1/2} - x_{i-1/2})$ for all i. If $\lambda_i^+(x)$ and $\lambda_i^-(x)$ are given by the relations (15), then the following approximations can be obtained*

$$\begin{aligned}
\int_{x_{i-1/2}}^{x_{i+1/2}} f(x)\,dx &= \int_{x_i}^{x_{i+1}} \lambda_i^+(x) f(x)\,dx + \int_{x_{i-1}}^{x_i} \lambda_i^-(x) f(x)\,dx \\
&\quad + \frac{f(x_i)}{2}\left[\Delta x_i - \left(\frac{\Delta x_{i-1} + \Delta x_{i+1}}{2}\right)\right] \\
&\quad - \frac{f'(x_i)}{12}\left[(\Delta x_{i+1} - \Delta x_{i-1})\left\{\Delta x_i + \left(\frac{\Delta x_{i-1} + \Delta x_{i+1}}{2}\right)\right\}\right] \\
&\quad + \mathcal{O}(\Delta x^3), \quad i = 2, \ldots, I-1, \\
\int_{x_{i-1/2}}^{x_{i+1/2}} f(x)\,dx &= \int_{x_{i-1}}^{x_i} \lambda_i^-(x) f(x)\,dx + \frac{f(x_i)}{2}\left[\Delta x_i - \Delta x_{i-1}\right] + \mathcal{O}(\Delta x^2), \quad i = I, \\
\int_{x_{i-1/2}}^{x_{i+1/2}} f(x)\,dx &= \int_{x_i}^{x_{i+1}} \lambda_i^+(x) f(x)\,dx + \frac{f(x_i)}{2}\left[\Delta x_i - \Delta x_{i+1}\right] + \mathcal{O}(\Delta x^2), \quad i = 1.
\end{aligned}$$

Proof Let us first take the cases $i = 2, \ldots I-1$ and for simplicity let us denote by $\mathfrak{I}_i$ the following expression

$$\mathfrak{I}_i(f) = \int_{x_{i-1/2}}^{x_{i+1/2}} f(x)\,dx - \left(\int_{x_i}^{x_{i+1}} \lambda_i^+(x) f(x)\,dx + \int_{x_{i-1}}^{x_i} \lambda_i^-(x) f(x)\,dx \right).$$

The application of Taylor series expansion of $f(x)$ about x_i in $\mathfrak{I}_i$ gives

$$\begin{aligned}\mathfrak{I}_i(f) = f(x_i) &\left[\Delta x_i - \left(\int_{x_i}^{x_{i+1}} \lambda_i^+(x)dx + \int_{x_{i-1}}^{x_i} \lambda_i^-(x)dx \right) \right] \\ &- f'(x_i) \left(\int_{x_i}^{x_{i+1}} \lambda_i^+(x)(x-x_i)dx + \int_{x_{i-1}}^{x_i} \lambda_i^-(x)(x-x_i)dx \right) + \mathcal{O}(\Delta x^3).\end{aligned}$$

Substituting the expression (15) of λ_i^+ and λ_i^- into the preceding equation, we obtain

$$\begin{aligned}\mathfrak{I}_i(f) = f(x_i) &\left[\Delta x_i - \frac{1}{2}(x_{i+1} - x_{i-1}) \right] \\ &- \frac{f'(x_i)}{6} \left[(x_{i+1} - x_{i-1}) \{ (x_{i+1} - x_i) - (x_i - x_{i-1}) \} \right] + \mathcal{O}(\Delta x^3). \end{aligned} \tag{18}$$

For the cell centered grids, i.e. $x_i = (x_{i-1/2} + x_{i+1/2})/2$, the Eq. (18) reduces to

$$\begin{aligned}\mathfrak{I}_i(f) = \frac{f(x_i)}{2} &\left[\Delta x_i - \frac{1}{2}(\Delta x_{i+1} + \Delta x_{i-1}) \right] \\ &- \frac{f'(x_i)}{12} \left[(\Delta x_{i+1} - \Delta x_{i-1}) \left\{ \Delta x_i + \left(\frac{\Delta x_{i-1} + \Delta x_{i+1}}{2} \right) \right\} \right] + \mathcal{O}(\Delta x^3).\end{aligned}$$

Now we consider $i = 1$ and $i = I$.

$$\mathfrak{I}_I(f) = \int_{I-1/2}^{I+1/2} f(x)dx - \int_{x_{I-1}}^{x_I} \lambda_I^-(x) f(x)dx.$$

Applying the midpoint and right triangular rules to the first and second terms respectively, we get

$$\begin{aligned}\mathfrak{I}_I(f) &= f(x_I)\Delta x_I - \lambda_I^-(x_I) f(x_I)(x_I - x_{I-1}) + \mathcal{O}(\Delta x^2)\\ &= f(x_I)\left[\Delta x_I - (x_I - x_{I-1})\right] + \mathcal{O}(\Delta x^2)\\ &= f(x_I)\left[\Delta x_I - \frac{1}{2}(\Delta x_I - \Delta x_{I-1})\right] + \mathcal{O}(\Delta x^2)\\ &= \frac{f(x_I)}{2}(\Delta x_I - \Delta x_{I-1}) + \mathcal{O}(\Delta x^2).\end{aligned}$$

Similarly we can obtain

$$\mathfrak{I}_1(f) = \frac{f(x_1)}{2}(\Delta x_1 - \Delta x_2) + \mathcal{O}(\Delta x^2).$$

Hence the lemma is proved. □

Let us first calculate the local discretization error of the integrated birth term. The integrated birth term is the following

$$B_i = \int_{x_{i-1/2}}^{x_{i+1/2}} \int_{x}^{x_{I+1/2}} b(x,\epsilon) S(\epsilon) n(t,\epsilon) d\epsilon dx.$$

Let us denote

$$f(t,x) = \int_{x}^{x_{I+1/2}} b(x,\epsilon) S(\epsilon) n(t,\epsilon) d\epsilon.$$

Considering $i = 2, \ldots, I-1$ and using Lemma 3.2, we can rewrite B_i as

$$\begin{aligned}B_i = &\int_{x_i}^{x_{i+1}} \lambda_i^+(x) \int_{x}^{x_{I+1/2}} b(x,\epsilon) S(\epsilon) n(t,\epsilon) d\epsilon dx\\ &+ \int_{x_{i-1}}^{x_i} \lambda_i^-(x) \int_{x}^{\epsilon} b(x,\epsilon) S(\epsilon) n(t,\epsilon) d\epsilon dx + \mathfrak{I}_i(f).\end{aligned}$$

Changing the order of integration of the first two terms on the right hand side, we obtain

$$
\begin{aligned}
B_i = & \int_{x_i}^{x_{i+1}} \int_{x_i}^{\epsilon} \lambda_i^+(x) b(x,\epsilon) S(\epsilon) n(t,\epsilon) dx d\epsilon \\
& + \int_{x_{i+1}}^{x_{I+1/2}} \int_{x_i}^{x_{i+1}} \lambda_i^+(x) b(x,\epsilon) S(\epsilon) n(t,\epsilon) dx d\epsilon \\
& + \int_{x_{i-1}}^{x_i} \int_{x_{i-1}}^{\epsilon} \lambda_i^-(x) b(x,\epsilon) S(\epsilon) n(t,\epsilon) dx d\epsilon \\
& + \int_{x_i}^{x_{I+1/2}} \int_{x_{i-1}}^{x_i} \lambda_i^-(x) b(x,\epsilon) S(\epsilon) n(t,\epsilon) dx d\epsilon + \Im_i(f).
\end{aligned}
$$

Each integral term on the right hand side can be further rewritten as

$$
\begin{aligned}
B_i = & \int_{x_i}^{x_{i+1/2}} \int_{x_i}^{\epsilon} \lambda_i^+(x) b(x,\epsilon) S(\epsilon) n(t,\epsilon) dx d\epsilon \\
& + \int_{x_{i+1/2}}^{x_{i+1}} \int_{x_i}^{\epsilon} \lambda_i^+(x) b(x,\epsilon) S(\epsilon) n(t,\epsilon) dx d\epsilon \\
& + \int_{x_{i+1}}^{x_{i+3/2}} \int_{x_i}^{x_{i+1}} \lambda_i^+(x) b(x,\epsilon) S(\epsilon) n(t,\epsilon) dx d\epsilon \\
& + \sum_{k=i+2}^{I} \int_{x_{k-1/2}}^{x_{k+1/2}} \int_{x_i}^{x_{i+1}} \lambda_i^+(x) b(x,\epsilon) S(\epsilon) n(t,\epsilon) dx d\epsilon \\
& + \int_{x_{i-1}}^{x_{i-1/2}} \int_{x_{i-1}}^{\epsilon} \lambda_i^-(x) b(x,\epsilon) S(\epsilon) n(t,\epsilon) dx d\epsilon \\
& + \int_{x_{i-1/2}}^{x_i} \int_{x_{i-1}}^{\epsilon} \lambda_i^-(x) b(x,\epsilon) S(\epsilon) n(t,\epsilon) dx d\epsilon \\
& + \int_{x_i}^{x_{i+1/2}} \int_{x_{i-1}}^{x_i} \lambda_i^-(x) b(x,\epsilon) S(\epsilon) n(t,\epsilon) dx d\epsilon \\
& + \sum_{k=i+1}^{I} \int_{x_{k-1/2}}^{x_{k+1/2}} \int_{x_{i-1}}^{x_i} \lambda_i^-(x) b(x,\epsilon) S(\epsilon) n(t,\epsilon) dx d\epsilon + \Im_i(f). \qquad (19)
\end{aligned}
$$

Let us denote the integral terms on the right hand side by $I_1, \ldots, I_8$ and simplify them separately

$$I_1 = \int_{x_i}^{x_{i+1/2}} \underbrace{\int_{x_i}^{\epsilon} \lambda_i^+(x) b(x,\epsilon) S(\epsilon) n(t,\epsilon) dx}_{=:g(t,\epsilon)} d\epsilon.$$

The Taylor series expansion of $g(t,\epsilon)$ with respect to ϵ about x_i gives

$$I_1 = g(t,x_i)\frac{\Delta x_i}{2} + g_\epsilon(t,x_i)\frac{\Delta x_i^2}{8} + \mathcal{O}(\Delta x^3), \tag{20}$$

where

$$g_\epsilon(t,x_i) = \frac{\partial g}{\partial \epsilon}(t,x_i) = \frac{\partial g}{\partial \epsilon}(t,\epsilon)|_{\epsilon=x_i}.$$

Let us calculate $g_\epsilon(t,x_i)$ using the Leibniz rule for differentiating under an integral

$$g_\epsilon(t,x_i) = \Bigg[n(t,\epsilon)S(\epsilon) \left\{ \int_{x_i}^{\epsilon} \lambda_i^+(x) b_\epsilon(x,\epsilon) dx + \lambda_i^+(\epsilon) b(\epsilon,\epsilon) \right\} + \{ n_\epsilon(t,\epsilon)S(\epsilon) + n(t,\epsilon)S_\epsilon(\epsilon) \} \int_{x_i}^{\epsilon} \lambda_i^+(x) b(x,\epsilon) dx \Bigg]_{\epsilon=x_i}.$$

All integral terms with $\epsilon = x_i$ vanish, this gives

$$g_\epsilon(t,x_i) = n(t,x_i)S(x_i)\lambda_i^+(x_i)b(x_i,x_i).$$

From the definition of λ_i^+ and λ_i^-, we have

$$\lambda_i^{\pm}(x_{i\pm k}) = \begin{cases} 0, & k = 1, \\ 1, & k = 0. \end{cases} \tag{21}$$

Thus we get $g_\epsilon(t,x_i)$ as

$$g_\epsilon(t,x_i) = n(t,x_i)S(x_i)b(x_i,x_i).$$

Substituting the value of $g_\epsilon(t,x_i)$ and also $g(t,x_i) = 0$ in the Eq. (20) we get

$$I_1 = b(x_i,x_i)S(x_i)n(t,x_i)\frac{\Delta x_i^2}{8} + \mathcal{O}(\Delta x^3).$$

Now we consider the second term

$$I_2 = \int_{x_{i+1/2}}^{x_{i+1}} g(t,\epsilon)d\epsilon.$$

Similarly as before, the application of Taylor series expansion simplifies the term as

$$I_2 = g(t,x_{i+1})\frac{\Delta x_{i+1}}{2} - g_\epsilon(t,x_{i+1})\frac{\Delta x_{i+1}^2}{8} + \mathcal{O}(\Delta x^3). \tag{22}$$

Here $g_\epsilon(t,x_{i+1})$ is given by

$$g_\epsilon(t,x_{i+1}) = \Bigg[n(t,\epsilon)S(\epsilon)\left\{\int_{x_i}^{\epsilon}\lambda_i^+(x)b_\epsilon(x,\epsilon)dx + \lambda_i^+(\epsilon)b(\epsilon,\epsilon)\right\} + \{n_\epsilon(t,\epsilon)S(\epsilon) + n(t,\epsilon)S_\epsilon(\epsilon)\}\int_{x_i}^{\epsilon}\lambda_i^+(x)b(x,\epsilon)dx\Bigg]_{\epsilon=x_{i+1}}.$$

Now we apply the left rectangle rule to get

$$g_\epsilon(t,x_{i+1}) = \Big[n(t,\epsilon)S(\epsilon)\left\{\lambda_i^+(x_i)b_\epsilon(x_i,\epsilon)(\epsilon-x_i) + \lambda_i^+(\epsilon)b(\epsilon,\epsilon)\right\} + \{n_\epsilon(t,\epsilon)S(\epsilon) + n(t,\epsilon)S_\epsilon(\epsilon)\}\lambda_i^+(x_i)b(x_i,\epsilon)(\epsilon-x_i)\Big]_{\epsilon=x_{i+1}}.$$

Using the expression (21) it can be further simplified as

$$g_\epsilon(t,x_{i+1}) = \Big[n(t,x_{i+1})S(x_{i+1})b_\epsilon(x_i,x_{i+1}) + \{n_\epsilon(t,x_{i+1})S(x_{i+1}) + n(t,x_{i+1})S_\epsilon(x_{i+1})\}b(x_i,x_{i+1})\Big]\left(\frac{\Delta x_i + \Delta x_{i+1}}{2}\right).$$

It follows that

$$g_\epsilon(t,x_{i+1}) = \mathcal{O}(\Delta x).$$

Substituting it into the Eq. (22) we obtain

$$\begin{aligned} I_2 &= g(t,x_{i+1})\frac{\Delta x_{i+1}}{2} + \mathcal{O}(\Delta x^3) \\ &= \frac{\Delta x_{i+1}}{2}S(x_{i+1})n(t,x_{i+1})\int_{x_i}^{x_{i+1}}\lambda_i^+(x)b(x,x_{i+1})dx + \mathcal{O}(\Delta x^3). \end{aligned}$$

The third and fourth terms can be simplified using the left rectangle and midpoint rule for the outer integral respectively to give

$$I_3 = \frac{\Delta x_{i+1}}{2} S(x_{i+1}) n(t, x_{i+1}) \int_{x_i}^{x_{i+1}} \lambda_i^+(x) b(x, x_{i+1}) dx + \mathcal{O}(\Delta x^3),$$

and

$$I_4 = \sum_{k=i+2}^{I} S(x_k) n(t, x_k) \Delta x_k \int_{x_i}^{x_{i+1}} \lambda_i^+(x) b(x, x_k) dx + \mathcal{O}(\Delta x^3).$$

The fifth term can be simplified as the first term to get

$$I_5 = \tilde{g}(t, x_{i-1}) \frac{\Delta x_{i-1}}{2} + \tilde{g}_\epsilon(t, x_{i-1}) \frac{\Delta x_i^2}{8} + \mathcal{O}(\Delta x^3), \tag{23}$$

where

$$\tilde{g}(t, \epsilon) = \int_{x_{i-1}}^{\epsilon} \lambda_i^-(x) b(x, \epsilon) S(\epsilon) n(t, \epsilon) dx.$$

The derivative $\tilde{g}_\epsilon(t, x_{i-1})$ is given by

$$\tilde{g}_\epsilon(t, x_{i-1}) = \Bigg[n(t, \epsilon) S(\epsilon) \left\{ \int_{x_{i-1}}^{\epsilon} \lambda_i^-(x) b_\epsilon(x, \epsilon) dx + \lambda_i^-(\epsilon) b(\epsilon, \epsilon) \right\} + \{ n_\epsilon(t, \epsilon) S(\epsilon) + n(t, \epsilon) S_\epsilon(\epsilon) \} \int_{x_{i-1}}^{\epsilon} \lambda_i^-(x) b(x, \epsilon) dx \Bigg]_{\epsilon = x_{i-1}}.$$

Since both integrals in the preceding equation with $\epsilon = x_{i-1}$ are zero and $\lambda_i^-(x_{i-1}) = 0$, this equation leads to

$$\tilde{g}_\epsilon(t, x_{i-1}) = 0.$$

Thus the term (23) can be written as

$$I_5 = 0 + \mathcal{O}(\Delta x^3).$$

Similarly the sixth term is given by

$$I_6 = \tilde{g}(t, x_i) \frac{\Delta x_i}{2} - \tilde{g}_\epsilon(t, x_i) \frac{\Delta x_i^2}{8} + \mathcal{O}(\Delta x^3), \tag{24}$$

where

$$\tilde{g}_\epsilon(t,x_i) = \Bigg[n(t,\epsilon)S(\epsilon)\left\{\int_{x_{i-1}}^{\epsilon} \lambda_i^-(x)b_\epsilon(x,\epsilon)dx + \lambda_i^-(\epsilon)b(\epsilon,\epsilon)\right\} + \{n_\epsilon(t,\epsilon)S(\epsilon) + n(t,\epsilon)S_\epsilon(\epsilon)\}\int_{x_{i-1}}^{\epsilon} \lambda_i^-(x)b(x,\epsilon)dx \Bigg]_{\epsilon=x_i}.$$

Since both integrals with $\epsilon = x_i$ are of order Δx, this equation leads to

$$\tilde{g}_\epsilon(t,x_i) = \mathcal{O}(\Delta x) + n(t,x_i)S(x_i)b(x_i,x_i) + \mathcal{O}(\Delta x).$$

Substituting $\tilde{g}_\epsilon(t,x_i)$ into the Eq. (24) we get

$$I_6 = \frac{\Delta x_i}{2}S(x_i)n(t,x_i)\int_{x_{i-1}}^{x_i} \lambda_i^-(x)b(x,x_i)dx - \frac{\Delta x_i^2}{8}n(t,x_i)S(x_i)b(x_i,x_i) + \mathcal{O}(\Delta x^3).$$

Similar to third and fourth term the last two terms using left triangular and midpoint rules can be simplified as

$$I_7 = \frac{\Delta x_i}{2}S(x_i)n(t,x_i)\int_{x_{i-1}}^{x_i} \lambda_i^-(x)b(x,x_i)dx + \mathcal{O}(\Delta x^3),$$

and

$$I_8 = \sum_{k=i+1}^{I} S(x_k)n(t,x_k)\Delta x_k \int_{x_{i-1}}^{x_i} \lambda_i^-(x)b(x,x_k)dx + \mathcal{O}(\Delta x^3).$$

Finally all these terms can be substituted in Eq. (19)

$$B_i = b(x_i,x_i)S(x_i)n(t,x_i)\frac{\Delta x_i^2}{8} + \frac{\Delta x_{i+1}}{2}S(x_{i+1})n(t,x_{i+1})\int_{x_i}^{x_{i+1}} \lambda_i^+(x)b(x,x_{i+1})dx + \frac{\Delta x_{i+1}}{2}S(x_{i+1})n(t,x_{i+1})\int_{x_i}^{x_{i+1}} \lambda_i^+(x)b(x,x_{i+1})dx + \sum_{k=i+2}^{I} S(x_k)n(t,x_k)\Delta x_k \int_{x_i}^{x_{i+1}} \lambda_i^+(x)b(x,x_k)dx$$

$$+\frac{\Delta x_i}{2}S(x_i)n(t,x_i)\int\limits_{x_{i-1}}^{x_i}\lambda_i^-(x)b(x,x_i)dx-\frac{\Delta x_i^2}{8}n(t,x_i)S(x_i)b(x_i,x_i)$$

$$+\frac{\Delta x_i}{2}S(x_i)n(t,x_i)\int\limits_{x_{i-1}}^{x_i}\lambda_i^-(x)b(x,x_i)dx$$

$$+\sum_{k=i+1}^{I}S(x_k)n(t,x_k)\Delta x_k\int\limits_{x_{i-1}}^{x_i}\lambda_i^-(x)b(x,x_k)dx+\mathcal{O}(\Delta x^3)+\mathfrak{I}_i(f). \tag{25}$$

It can be further simplified as

$$B_i=\sum_{k=i+1}^{I}S(x_k)n(t,x_k)\Delta x_k\int\limits_{x_i}^{x_{i+1}}\lambda_i^+(x)b(x,x_k)dx$$

$$+\sum_{k=i}^{I}S(x_k)n(t,x_k)\Delta x_k\int\limits_{x_{i-1}}^{x_i}\lambda_i^-(x)b(x,x_k)dx+\mathcal{O}(\Delta x^3)+\mathfrak{I}_i(f).$$

Furthermore we can use the relationship $N_i=n(t,x_i)\Delta x_i+\mathcal{O}(\Delta x_i^3)$ for the midpoint rule to get the form

$$B_i=\sum_{k=i+1}^{I}S(x_k)N_k(t)\int\limits_{x_i}^{x_{i+1}}\lambda_i^+(x)b(x,x_k)dx$$

$$+\sum_{k=i}^{I}S(x_k)N_k(t)\int\limits_{x_{i-1}}^{x_i}\lambda_i^-(x)b(x,x_k)dx+\mathcal{O}(\Delta x^3)+\mathfrak{I}_i(f).$$

The first two terms on the right hand side are exactly the fixed pivot discretization i.e.,

$$B_i=\hat{B}_i^{\mathrm{FP}}+\mathcal{O}(\Delta x^3)+\mathfrak{I}_i(f).$$

After substituting the value of $\mathfrak{I}_i(f)$ we get

$$B_i=\hat{B}_i^{\mathrm{FP}}+\frac{f(x_i)}{2}\left[\Delta x_i-\frac{1}{2}\left(\Delta x_{i+1}+\Delta x_{i-1}\right)\right]$$

$$-\frac{f'(x_i)}{12}\left[\left(\Delta x_{i+1}-\Delta x_{i-1}\right)\left\{\Delta x_i+\left(\frac{\Delta x_{i-1}+\Delta x_{i+1}}{2}\right)\right\}\right]+\mathcal{O}(\Delta x^3). \tag{26}$$

Now we consider the birth term for $i = 1$

$$B_1 = \int_{x_{1-1/2}}^{x_{1+1/2}} \int_{x}^{x_{I+1/2}} b(x,\epsilon) S(\epsilon) n(t,\epsilon) d\epsilon dx.$$

Using the Lemma 3.2, the birth term can be rewritten as

$$B_1 = \int_{x_1}^{x_2} \lambda_1^+(x) \int_{x}^{x_{I+1/2}} b(x,\epsilon) S(\epsilon) n(t,\epsilon) d\epsilon \, dx + \Im_1(f).$$

Changing the order of integration we get

$$\begin{aligned} B_1 = & \int_{x_1}^{x_2} \int_{x_1}^{\epsilon} \lambda_1^+(x) b(x,\epsilon) S(\epsilon) n(t,\epsilon) dx d\epsilon. \\ & + \int_{x_2}^{x_{I+1/2}} \int_{x_1}^{x_2} \lambda_1^+(x) b(x,\epsilon) S(\epsilon) n(t,\epsilon) dx d\epsilon + \Im_1(f). \end{aligned}$$

We break up the integration as follows

$$\begin{aligned} B_1 = & \int_{x_1}^{x_{2-1/2}} \int_{x_1}^{\epsilon} \lambda_1^+(x) b(x,\epsilon) S(\epsilon) n(t,\epsilon) dx d\epsilon \\ & + \int_{x_{2-1/2}}^{x_2} \int_{x_1}^{\epsilon} \lambda_1^+(x) b(x,\epsilon) S(\epsilon) n(t,\epsilon) dx d\epsilon \\ & + \int_{x_2}^{x_{2+1/2}} \int_{x_1}^{x_2} \lambda_1^+(x) b(x,\epsilon) S(\epsilon) n(t,\epsilon) dx d\epsilon \\ & + \sum_{k=3}^{I} \int_{x_{k-1/2}}^{x_{k+1/2}} \int_{x_1}^{x_2} \lambda_1^+(x) b(x,\epsilon) S(\epsilon) n(t,\epsilon) dx d\epsilon + \Im_1(f). \end{aligned}$$

Application of the left, right, left rectangular and midpoint rules to the outer integration in the first, second, third and fourth integral terms respectively we obtain

$$\begin{aligned} B_1 = 0 &+ \frac{\Delta x_2}{2} \int_{x_1}^{x_2} \lambda_1^+(x) b(x, x_2) S(x_2) n(t, x_2) dx \\ &+ \frac{\Delta x_2}{2} \int_{x_1}^{x_2} \lambda_1^+(x) b(x, x_2) S(x_2) n(t, x_2) dx \\ &+ \sum_{k=3}^{I} \Delta x_k \int_{x_1}^{x_2} \lambda_1^+(x) b(x, x_k) S(x_k) n(t, x_k) dx + \mathcal{O}(\Delta x^2) + \mathfrak{I}_1(f). \end{aligned}$$

We can rewrite this in a more simplified form as

$$\begin{aligned} B_1 &= N_2(t) S(x_2) \int_{x_1}^{x_2} \lambda_1^+(x) b(x, x_2) dx \\ &\quad + \sum_{k=3}^{I} N_k(t) S(x_k) \int_{x_1}^{x_2} \lambda_1^+(x) b(x, x_k) dx + \mathcal{O}(\Delta x^2) + \mathfrak{I}_I(f) \\ &= \sum_{k=2}^{I} N_k(t) S(x_k) \int_{x_1}^{x_2} \lambda_1^+(x) b(x, x_k) dx + \mathcal{O}(\Delta x^2) + \mathfrak{I}_1(f). \end{aligned}$$

In terms of fixed pivot discretization we have

$$B_1 = \hat{B}_1^{\mathrm{FP}} + \frac{f(x_1)}{2} (\Delta x_1 - \Delta x_2) + \mathcal{O}(\Delta x^2). \tag{27}$$

Finally we consider the boundary cells $i = I$

$$B_I = \int_{x_{I-1/2}}^{x_{I+1/2}} \int_{x}^{x_{I+1/2}} b(x, \epsilon) S(\epsilon) n(t, \epsilon) d\epsilon dx.$$

$$B_I = \int_{x_{I-1}}^{x_I} \lambda_I^-(x) \int_{x}^{x_{I+1/2}} b(x, \epsilon) S(\epsilon) n(t, \epsilon) d\epsilon dx + \mathfrak{I}_I(f).$$

Changing the order of integration gives

$$B_I = \int_{x_{I-1}}^{x_I} \int_{x_{I-1}}^{\epsilon} \lambda_I^-(x) b(x,\epsilon) S(\epsilon) n(t,\epsilon) dx d\epsilon + \int_{x_I}^{x_{I+1/2}} \int_{x_{I-1}}^{x_I} \lambda_I^-(x) b(x,\epsilon) S(\epsilon) n(t,\epsilon) dx d\epsilon + \mathfrak{I}_I(f).$$

We break the first integral into two parts as

$$B_I = \int_{x_{I-1}}^{x_{I-1/2}} \int_{x_{I-1}}^{\epsilon} \lambda_I^-(x) b(x,\epsilon) S(\epsilon) n(t,\epsilon) dx d\epsilon + \int_{x_{I-1/2}}^{x_I} \int_{x_{I-1}}^{\epsilon} \lambda_I^-(x) b(x,\epsilon) S(\epsilon) n(t,\epsilon) dx d\epsilon + \int_{x_I}^{x_{I+1/2}} \int_{x_{I-1}}^{x_I} \lambda_I^-(x) b(x,\epsilon) S(\epsilon) n(t,\epsilon) dx d\epsilon + \mathfrak{I}_I(f).$$

Applying the left, right and left triangular rules into the first, second and third integration terms respectively to get

$$\begin{aligned} B_I &= 0 + \frac{\Delta x_I}{2} \int_{x_{I-1}}^{x_I} \lambda_I^-(x) b(x, x_I) S(x_I) n(t, x_I) dx. \\ &\quad + \frac{\Delta x_I}{2} \int_{x_{I-1}}^{x_I} \lambda_I^-(x) b(x, x_I) S(x_I) n(t, x_I) dx + \mathcal{O}(\Delta x^2) + \mathfrak{I}_I(f) \\ &= N_I(t) S(x_I) \int_{x_{I-1}}^{x_I} \lambda_I^-(x) b(x, x_I) dx + \mathcal{O}(\Delta x^2) + \mathfrak{I}_I(f). \end{aligned}$$

Again in terms of fixed pivot technique we obtain

$$B_I = \hat{B}_I^{\mathrm{CA}} + \frac{f(x_I)}{2} (\Delta x_I - \Delta x_{I-1}) + \mathcal{O}(\Delta x^2). \tag{28}$$

The local discretization error can be obtained by using midpoint rule as

$$D_i = S(x_i) N_i(t) + \mathcal{O}(\Delta x^3) = \hat{D}_i^{\mathrm{FP}} + \mathcal{O}(\Delta x^3). \tag{29}$$

Finally from the Eqs. (26), (27), (28) and (29), we can summarize the spatial truncation error $\sigma_i(t) = B_i - D_i - (\hat{B}_i^{\mathrm{FP}} - \hat{D}_i^{\mathrm{FP}})$ as follows

$$\sigma_1 = \frac{f(x_1)}{2}(\Delta x_1 - \Delta x_2) + \mathcal{O}(\Delta x^2), \tag{30}$$

$$\sigma_i = \frac{f(x_i)}{2}\left[\Delta x_i - \frac{1}{2}(\Delta x_{i+1} + \Delta x_{i-1})\right] - \frac{f'(x_i)}{12}\left[(\Delta x_{i+1} - \Delta x_{i-1})\left\{\Delta x_i + \left(\frac{\Delta x_{i-1} + \Delta x_{i+1}}{2}\right)\right\}\right] + \mathcal{O}(\Delta x^3), \quad i = 2, \ldots, I-1, \tag{31}$$

$$\sigma_I = \frac{f(x_I)}{2}(\Delta x_I - \Delta x_{I-1}) + \mathcal{O}(\Delta x^2). \tag{32}$$

Now we will evaluate the order of local truncation error on four different types of meshes:

3.1.1 Type A: *uniform mesh*

Let us first consider uniform mesh i.e. $\Delta x_i = \Delta x$. From the Eqs. (30–32) we have

$$\sigma_i(t) = \begin{cases} \mathcal{O}(\Delta x^2), & i = 1, I \\ \mathcal{O}(\Delta x^3), & i = 2, \ldots, I-1. \end{cases}$$

The order of consistency is given by

$$\begin{aligned} \|\sigma(t)\| &= |\sigma_1(t)| + \sum_{i=2}^{I-1} |\sigma_i(t)| + |\sigma_I(t)| \\ &= \mathcal{O}(\Delta x^2). \end{aligned}$$

So the technique is second order consistent on a uniform mesh.

3.1.2 Type B: *non-uniform smooth mesh*

If we assume grids to be smooth in the sense that $\Delta x_i - \Delta x_{i-1} = \mathcal{O}(\Delta x^2)$ and $2\Delta x_i - (\Delta x_{i-1} + \Delta x_{i+1}) = \mathcal{O}(\Delta x^3)$, where Δx is the maximum mesh width, then similarly to the uniform case we again have second order accuracy. Such grids can be obtained by some smooth transformation from uniform grids. Let us consider a variable ξ with uniform grids and a smooth transformation $x = g(\xi)$ to get

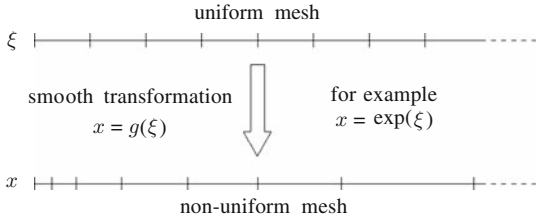

Fig. 2 Non-uniform smooth mesh

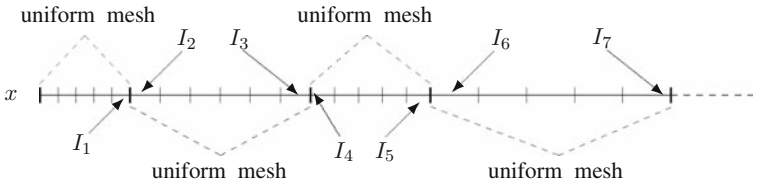

Fig. 3 Locally uniform smooth mesh

non-uniform smooth mesh, see Fig. 2. In this case the Eq. (30–32) can be simplified as

$$\begin{aligned}\sigma_1 &= \frac{f(x_1)}{2}\left[\Delta x_1 - \Delta x_2\right] + \mathcal{O}(\Delta x^2)\\ &= \frac{f(x_1)}{2}\left[\left\{g(\xi_{1+1/2}) - g(\xi_{1-1/2})\right\} - \left\{g(\xi_{2+1/2}) - g(\xi_{2-1/2})\right\}\right] + \mathcal{O}(h^2)\\ &= \frac{f(x_1)}{2}\left[g(\xi_1 + h/2) - g(\xi_1 - h/2) - g(\xi_1 + 3h/2) + g(\xi_1 + h/2)\right] + \mathcal{O}(h^2).\end{aligned}$$

Here h is the uniform mesh width in the ξ variable. Application of Taylor series expansion gives

$$\sigma_1 = \mathcal{O}(h^2).$$

Similarly we can prove that

$$\sigma_I = \mathcal{O}(h^2) \quad \text{and} \quad \sigma_i = \mathcal{O}(h^3).$$

Finally, analogously to the uniform mesh we get second order consistency here. An example of such smooth grids, commonly used in particle technology, are the so called geometric grids $x_{i+1/2} = r x_{i-1/2}$, $r > 1, i = 1, \ldots I$ or grids uniform on a logarithmic scale. These grids can be obtained by taking smooth transformation as exponential function. In this case we get $x_{i+1/2} = \exp(\xi_{i+1/2}) = \exp(h + \xi_{i-1/2}) = \exp(h)\exp(\xi_{i-1/2}) = \exp(h)x_{i-1/2} =: r x_{i-1/2}$, $r > 1$.

3.1.3 Type C: locally uniform mesh

An example of a locally uniform mesh is considered in Fig. 3. Let us consider that the computation domain is divided into finitely many sub-domains and in each

sub-domain is divided into an equal size mesh. In this way we have a locally uniform mesh. In each cell except boundaries of every sub-domain we have third order accuracy due to uniform mesh in each sub-domain. All boundaries of sub-domains except the outer boundaries of the first and last cell we have first order accuracy. This is due to the abrupt change in size at this boundary. At the first (last) outer boundary we obtain a second order accuracy as in the case of a uniform as well as non-uniform smooth mesh. For the example shown in the Fig. 3 we have

$$\sigma_i(t) = \begin{cases} \mathcal{O}(\Delta x), & i = I_1, I_2, \dots \\ \mathcal{O}(\Delta x^2), & i = 1, I, \\ \mathcal{O}(\Delta x^3), & \text{otherwise.} \end{cases}$$

Therefore we have

$$\begin{aligned} \|\sigma(t)\| &= |\sigma_1(t)| + |\sigma_I(t)| + \left(|\sigma_{I_1}(t)| + |\sigma_{I_2}(t)| + \cdots\right) + \sum_{\substack{j=2 \\ j \neq I_1, I_2, \dots}}^{I-1} |\sigma_j(t)| \\ &= \mathcal{O}(\Delta x). \end{aligned}$$

Thus in this case we get only first order consistency.

3.1.4 Type D: *non-uniform random mesh*

Finally we analyze the scheme for random grids. Since no cancellation takes place in the leading error terms of Eqs. (30–32) we have

$$\sigma_i(t) = \mathcal{O}(\Delta x),\ i = 1, \dots, I, \quad \text{and} \quad \|\sigma(t)\| = \mathcal{O}(1).$$

Thus the method is inconsistent on non-uniform random meshes.

3.2 Stability and convergence

The stability can be proved using the logarithmic norm defined by the Eq. (12). Here we evaluate the logarithmic norm of the matrix $\mathbf{A}$ from (17) as

$$\tilde{\mu}_1(\mathbf{A}) = \max_j \left(Re(a_{jj}) + \sum_{i \neq j} |a_{ij}| \right).$$

Since all elements of the matrix $\mathbf{A}$ are real and all non-diagonal elements are non-negative, the logarithmic norm can again be rewritten using (17) as

$$\begin{aligned}\tilde{\mu}_1(\mathbf{A}) &= \max_j \left(\sum_{1\le i\le I} a_{ij} \right) = \max_j \left(\sum_{i=1}^{j} \eta_{ij} S_j - S_j \right) \\ &= \max_j \left[S_j \left(\sum_{i=1}^{j} \eta_{ij} - 1 \right) \right]. \end{aligned} \tag{33}$$

The sum appearing in the above equation can be calculated as

$$\sum_{i=1}^{j} \eta_{ij} = \sum_{i=1}^{j} \int_{x_i}^{x_{i+1}} \lambda_i^+(x) b(x, x_j)\, dx + \sum_{i=2}^{j} \int_{x_{i-1}}^{x_i} \lambda_i^-(x) b(x, x_j)\, dx$$

Using the fact that $b(x, y) = 0$ for $x > y$ we get

$$\begin{aligned}\sum_{i=1}^{j} \eta_{ij} &= \sum_{i=1}^{j-1} \int_{x_i}^{x_{i+1}} \lambda_i^+(x) b(x, x_j)\, dx + \sum_{i=2}^{j} \int_{x_{i-1}}^{x_i} \lambda_i^-(x) b(x, x_j)\, dx \\ &= \sum_{i=1}^{j-1} \int_{x_i}^{x_{i+1}} \lambda_i^+(x) b(x, x_j)\, dx + \sum_{i=1}^{j-1} \int_{x_i}^{x_{i+1}} \lambda_{i+1}^-(x) b(x, x_j)\, dx \\ &= \sum_{i=1}^{j-1} \int_{x_i}^{x_{i+1}} \left[\lambda_i^+(x) + \lambda_{i+1}^-(x) \right] b(x, x_j)\, dx. \end{aligned}$$

Using the properties $\lambda_i^+(x) + \lambda_{i+1}^-(x) = 1$ and of the breakage function (2), we get

$$\begin{aligned}\sum_{i=1}^{j} \eta_{ij} &= \sum_{i=1}^{j-1} \int_{x_i}^{x_{i+1}} b(x, x_j)\, dx \\ &= \int_{x_1}^{x_j} b(x, x_j)\, dx \\ &= \int_{0}^{x_j} b(x, x_j)\, dx - \int_{0}^{x_1} b(x, x_j)\, dx \\ &= \nu(x_j) - \epsilon(x_1, x_j). \end{aligned}$$

Note that $\epsilon(x_1, x_j) > 0$ is a small value and $\lim_{x_1 \to 0} \epsilon(x_1, x_j) = 0$. Substituting the above sum into the Eq. (33), we obtain

$$\begin{aligned}\tilde{\mu}_1(\mathbf{A}) &= \max_j \left[S_j \left(\nu(x_j) - \epsilon(x_1, x_j) - 1 \right) \right] \\ &\leq \max_j \left[S_j \nu(x_j) \right] \leq \max_{x \in \Omega} S(x)\nu(x) =: \omega.\end{aligned}$$

Application of Theorem 2.4 provides the bound

$$\|e^{t\mathbf{A}}\| \leq e^{t\omega}.$$

This shows the stability of the fixed pivot technique with the stability constant ω. Thus, from Theorem 2.6 we have convergence of order p with error bounds

$$\|\epsilon(t)\| = C_0 e^{\omega t} \Delta x^p + \frac{C}{\omega} \left(e^{\omega t} - 1 \right) \Delta x^p, \quad 0 \leq t \leq T,$$

with constants $C, C_0 > 0$. Here p is the order of consistency discussed in previous section and Δx is the maximum mesh width. As discussed in Sect. 3.1, p could be 0, 1 or 2 depending on the type of mesh used for the computation.

4 Numerical examples

We now verify our mathematical observations on the convergence by numerical examples. Each case discussed above has been considered separately. For detailed comparisons of numerical results on number density and moments with analytical solutions, readers are referred to Kumar and Ramkrishna [16]. All numerical simulations below will be carried out to investigate the experimental order of convergence.

We shall now turn our attention to a suitable ODE solver to solve the resulting set of ODEs. When integrating the resultant system (16) using a standard ODE routine, for example the ODE45, ODE15S solvers in MATLAB, this may lead to negative values for the number density at large sizes. These negative values may lead in consequence to instabilities of the whole system. Therefore, one should take care of the positivity of the solution by the numerical integration routine. We force the positivity in our numerical results using an adaptive time step Runge–Kutta method. The step-size adjustment algorithm is based on embedded Runge–Kutta formulas, originally invented by Fehlberg. It uses a fifth-order method with six functions evaluation where another combination of the six functions gives a fourth order method. The difference between the two estimates is used as an estimate of the truncation error to adjust the step size. A more detailed description of the method and information about implementation can be found in [24].

Let us first calculate the experimental order of convergence for uniform meshes. For a uniform mesh, we consider the following normally distributed initial condition

$$n(0, x) = \frac{1}{\sigma\sqrt{2\pi}} \exp\left[-\frac{(x - \mu)^2}{2\sigma^2} \right]. \tag{34}$$

Table 1 Uniform grids

Grids points	Relative error L_1	EOC
60	–	–
120	0.0343	–
240	9.6E−3	1.83
480	2.5E−3	1.92
960	6.5E−4	1.97

Note that due to the highly steep nature of the exponential function, an exponentially decreasing initial condition is not suitable for uniform grids. Furthermore, we have considered the following breakage and selection functions

$$b(x, y) = \frac{12x}{y^2}\left(1 - \frac{x}{y}\right), \qquad S(x) = S_0 x^2. \tag{35}$$

Since analytical solutions are not available for the above initial condition and breakage kernels we use the following formula in order to calculate the experimental order of convergence

$$\text{EOC} = \ln\left(\frac{\|\hat{\mathbf{N}}_h - \hat{\mathbf{N}}_{h/2}\|}{\|\hat{\mathbf{N}}_{h/2} - \hat{\mathbf{N}}_{h/4}\|}\right) \Big/ \ln(2). \tag{36}$$

Here $\hat{\mathbf{N}}_h$ denotes numerical results taken using mesh width h. For the numerical computation we have taken the minimum and maximum values of x as 0 and 1 respectively. The other parameters are $\sigma^2 = 0.01$, $\mu = 0.5$ and $S_0 = 1$. The computation time t is set to be 200 (breakage extent ≈ 11.78). The numerical results are presented in Table 1. As expected from the mathematical analysis, numerical results show convergence of second order.

Now we consider the second case of non-uniform smooth meshes. As mentioned before such a mesh can be obtained by some smooth transformation from a uniform mesh. Here we have considered the exponential transformation as $x = \exp(\xi)$, where ξ is the variable for which we have the uniform mesh. Such a mesh is also known as geometric mesh. In this case we take an exponentially decreasing function, $\exp(-x)$ as initial condition. The linear selection function $S(x) = x$ and uniform binary breakage $b(x, y) = 2/y$ are considered. Here, we take t = 10 (breakage extent $\approx$ 11) in our numerical results. The computational domain in this case is taken as $[1e-6, 150]$ which corresponds to the ξ domain $[\ln(1e-6), \ln(150)]$. It should be noted that any small positive real number can be chosen as the minimum value of x. However, we have taken it to be $1e-6$. The analytical solution for this case can be found in Ziff and McGrady [28]. Since the analytical solution is known, the experimental order of convergence can be calculated as

$$\text{EOC} = \ln(E_1/E_{2l})/\ln(2), \tag{37}$$

Table 2 Non-uniform smooth grids

Grids points	Relative error L_1	EOC
60	0.0307	–
120	7.6E−3	2.01
240	1.9E−3	2.01
480	4.6E−4	2.05

Table 3 Locally uniform grid

Grids points	Relative error L_1	EOC
60	0.1938	–
120	0.1037	0.90
240	0.0522	0.99
480	0.0259	1.01

where E_I and E_{2I} are the L_1 error norms. The symbols I and $2I$ correspond to the degrees of freedom. The numerical results have been summarized in Table 2. The relative error has been calculated by dividing the error $\|\mathbf{N} - \hat{\mathbf{N}}\|$ by $\|\mathbf{N}\|$. Once again numerical results show that the fixed pivot technique give second order accuracy on non-uniform smooth mesh.

The third test case has been performed on a locally uniform mesh using the same problem and the same computational parameters as in the previous case. In this case we started the computation on 30 geometric meshes and then each cell was divided into two equal parts in further level of computation. In this way we obtained a locally uniform mesh. The EOC has been summarized in Table 3. As expected, the table clearly shows that the fixed pivot technique is only first order accurate.

Finally we consider the fourth case of non-uniform random mesh. Similar to the third and second cases, computations have been performed on the same problem. Computations have been performed using two different types of random grids. Since we require more refined grids at small x values due to the exponential initial condition, we use more refined grids at small volume range. In type-I grids we started again with the 30 geometric meshes and then each cell was divided into two parts of random width in further levels of computation. For each value of $I = 60, 120, 240, 480$, we performed 10 runs on different random grids and the relative L_1 errors were measured. The mean of these errors over 10 runs is used to calculate the EOC. The numerical results have been shown in Table 4(a). For the second type of grids, referred to as type-II, we first generate 480 random grids and then further levels of grids (240, 120, 60) were extracted from these random grids by selecting alternative grid points. This process was repeated 10 number of times and the relative L_1 error was measured for each value of $I = 60, 120, 240, 480$. Again, the mean of these errors over 10 runs is used to calculate the EOC shown in Table 4(b). Clearly Table 4 shows that the fixed pivot technique is not convergent. As can be seen from the table, the relative L_1 error increases with finer grids.

Table 4 Non-uniform random grids

Grids points	Error L_1	EOC
(a) Type I		
60	0.0668	–
120	0.0960	−0.52
240	0.1516	−0.66
480	0.1758	−0.21
(b) Type II		
60	0.0693	–
120	0.1267	−0.87
240	0.1462	−0.21
480	0.1688	−0.21

5 Conclusions

A complete convergence analysis of the fixed pivot has been obtained for pure breakage population balance equation. It has been observed that the order of convergence depends on the type of grids chosen for the computation. The technique converges with second order on uniform and non-uniform smooth grids. However, it has been shown that the technique is only first order convergent on locally uniform grids. Finally, the scheme has been analyzed on non-uniform random grids and it has been found that the technique is not convergent. Moreover, all observations have been verified numerically. In a sequel to this paper, Kumar and Warnecke [14], we show how the cell average technique [13] has a better performance on non-uniform meshes.

Acknowledgments The authors wish to thank the reviewers for their comments and suggestions that helped to improve the manuscript.

References

1. Ball, J.M., Carr, J.: The discrete coagulation-fragmentation equations: Existence, uniqueness, and density conservation. J. Stat. Phys. **61**, 203–234 (1990)
2. Costa, F.P.D.: A finite-dimensional dynamical model for gelation in coagulation processes. J. Nonlin. Sci. **8**, 619–653 (1998)
3. Dubovskiĭ, P.B., Galkin, V.A., Stewart, I.W.: Exact solutions for the coagulation-fragmentation equations. J. Phys. A Math. Gen. **25**, 4737–4744 (1992)
4. Dubovskiĭ, P.B., Stewart, I.W.: Existence, uniqueness and mass conservation for the coagulation-fragmentation equation. Math. Meth. Appl. Sci. **19**, 571–591 (1996)
5. Everson, R.C., Eyre, D., Campbell, Q.P.: Spline method for solving continuous batch grinding and similarity equations. Comput. Chem. Eng. **21**, 1433–1440 (1997)
6. Filbet, F., Laurençot, P.: Mass-conserving solutions and non-conservative approximation to the smoluchowski coagulation equation. Archiv der Mathematik **83**, 558–567 (2004)
7. Hill, P.J., Ng, K.M.: New discretization procedure for the breakage equation. AIChE J. **41**, 1204–1216 (1995)
8. Hundsdorfer, W., Verwer, J.G.: Numerical solution of time-dependent advection–diffusion-reaction equations, 1st edn. Springer, New York (2003)

9. Kostoglou, M., Karabelas, A.J.: An assessment of low-order methods for solving the breakage equation. Powder Technol. **127**, 116–127 (2002)
10. Kostoglou, M., Karabelas, A.J.: Optimal low order methods of moments for solving the fragmentation equation. Powder Technol. **143**(144), 280–290 (2004)
11. Kostoglou, M., Karabelas, A.J.: On the self similar solution of fragmentation equation: Numerical evaluation with implication for the inverse problem. J. Colloid Interface Sci. **284**, 571–581 (2005)
12. Kumar, J., Peglow, M., Warnecke, G., Heinrich, S.: An efficient numerical technique for solving population balance equation involving aggregation, breakage, growth and nucleation. Powder Technol. **179**, 205–228 (2007)
13. Kumar, J., Peglow, M., Warnecke, G., Heinrich, S., Mörl, L.: Improved accuracy and convergence of discretized population balance for aggregation: the cell average technique. Chem. Eng. Sci. **61**, 3327–3342 (2006)
14. Kumar, J., Warnecke, G.: Convergence analysis of sectional methods for solving breakage population balance equation-II. The cell average technique. Accepted for publication in Numerische Mathematik (2008)
15. Kumar, J., Warnecke, G., Peglow, M., Heinrich, S.: Comparison of numerical methods for solving population balance equations incorporating aggregation and breakage. Powder Technol. (in press, 2008)
16. Kumar, S., Ramkrishna, D.: On the solution of population balance equations by discretization-I. A fixed pivot technique. Chem. Eng. Sci. **51**, 1311–1332 (1996)
17. Kumar, S., Ramkrishna, D.: On the solution of population balance equations by discretization-II. A moving pivot technique. Chem. Eng. Sci. **51**, 1333–1342 (1996)
18. Lamb, W.: Existence and uniqueness results for the continuous coagulation and fragmentation equation. Math. Meth. Appl. Sci. **27**, 703–721 (2004)
19. Laurençot, P.: On a class of continuous coagulation–fragmentation equations. J. Diff. Eq. **167**, 245–274 (2000)
20. Lee, M.H.: On the validity of the coagulation equation and the nature of runaway growth. Icarus **143**, 74–86 (2000)
21. McLaughlin, D.J., Lamb, W., McBride, A.C.: An existence and uniqueness result for a coagulation and multiple-fragmentation equation. SIAM J. Math. Anal. **28**, 1173–1190 (1997)
22. McLaughlin, D.J., Lamb, W., McBride, A.C.: Existence and uniqueness results for the non-autonomous coagulation and multiple-fragmentation equation. Math. Meth. Appl. Sci. **21**, 1067–1084 (1998)
23. Mishra, B.K.: Monte Carlo simulation of particle breakage process during grinding. Powder Technol. **110**, 246–252 (2000)
24. Press, W.H., Teukolsky, S.A., Vetterling, W.T., Flannery, B.P.: Numerical recipes in C++, 2nd edn. Cambridge University Press, The Edinburgh Building, Cambridge (2002)
25. Vanni, M.: Discretization procedure for the breakage equation. AIChE J. **45**, 916–919 (1999)
26. Vanni, M.: Approximate population balance equations for aggregation-breakage processes. J. Collid Interface Sci. **221**, 143–160 (2002)
27. Ziff, R.M.: New solution to the fragmentation equation. J. Phys. A Math. Gen. **24**, 2821–2828 (1991)
28. Ziff, R.M., McGrady, E.D.: The kinetics of cluster fragmentation and depolymerization. J. Phys. A Math. Gen. **18**, 3027–3037 (1985)